Please cite this article in press as: Lynch et al., Transitioning to confined spaces impacts bacterial swimming and escape response, Biophysical Journal (2022), https://doi.org/10.1016/j.bpj.2022.04.008

Biophysical *Journal*
Article

Biophysical Society

Transitioning to confined spaces impacts bacterial swimming and escape response

Jonathan B. Lynch,[1,*] Nicholas James,[2] Margaret McFall-Ngai,[1] Edward G. Ruby,[1] Sangwoo Shin,[3,4] and Daisuke Takagi[1,3,5]

[1]Pacific Biosciences Research Center, University of Hawai'i at Mānoa, Honolulu, Hawai'i; [2]Department of Cell and Molecular Biology, University of Hawai'i at Mānoa, Honolulu, Hawai'i; [3]Department of Mechanical Engineering, University of Hawai'i at Mānoa, Honolulu, Hawai'i; [4]Department of Mechanical and Aerospace Engineering, University at Buffalo, Buffalo, New York; and [5]Department of Mathematics, University of Hawai'i at Mānoa, Honolulu, Hawai'i

ABSTRACT Symbiotic bacteria often navigate complex environments before colonizing privileged sites in their host organism. Chemical gradients are known to facilitate directional taxis of these bacteria, guiding them toward their eventual destination. However, less is known about the role of physical features in shaping the path the bacteria take and defining how they traverse a given space. The flagellated marine bacterium *Vibrio fischeri*, which forms a binary symbiosis with the Hawaiian bobtail squid, *Euprymna scolopes*, must navigate tight physical confinement during colonization, squeezing through a tissue bottleneck constricting to ~2 μm in width on the way to its eventual home. Using microfluidic in vitro experiments, we discovered that *V. fischeri* cells alter their behavior upon entry into confined space, straightening their swimming paths and promoting escape from confinement. Using a computational model, we attributed this escape response to two factors: reduced directional fluctuation and a refractory period between reversals. Additional experiments in asymmetric capillary tubes confirmed that *V. fischeri* quickly escape from confined ends, even when drawn into the ends by chemoattraction. This avoidance was apparent down to a limit of confinement approaching the diameter of the cell itself, resulting in a balance between chemoattraction and evasion of physical confinement. Our findings demonstrate that nontrivial distributions of swimming bacteria can emerge from simple physical gradients in the level of confinement. Tight spaces may serve as an additional, crucial cue for bacteria while they navigate complex environments to enter specific habitats.

SIGNIFICANCE Symbiotic bacteria that navigate to and through specific host tissues often face tight physical confinement. This work reveals that confinement-associated changes in swimming can dramatically alter how bacteria move through environments, shaping bacterial localization in conjuncture with other motility-directing cues. This work helps explain how bacteria can avoid getting stuck in confined areas while transiting to privileged spaces, adding confinement as an environmental cue that symbiotic bacteria use to shape their motility behavior. In addition to guiding how bacteria move about in their host environment, these results about confinement-associated swimming behaviors could also be exploited for cell sorting in industrial settings.

INTRODUCTION

Motility is essential to the physiology of many bacteria. One of the most common modes of bacterial motility is coordinated rotation of extended structures called flagella, which utilize physical anisotropy to propel cells through viscous fluids (1,2). Coordination of flagellar rotation results in directional movement and, when combined with detection of physical and chemical cues, enables bacteria to migrate to or from particular sites, facilitating activities such as predation (3), accessing preferred niches (4,5), and pathogenesis (6). The directionality of flagellar swimming has been classically described in *Escherichia coli* by the "run-and-tumble" model (7), but flagella are also involved in other motility strategies, such as flicking (8,9) and wrapping (10,11). These swimming modalities each involve different specific flagellar actions, and their effects on cellular behavior depend on physical characteristics of the cell's environment, with seemingly straightforward changes in environment drastically shaping overall bacterial behavior (12).

Submitted November 16, 2021, and accepted for publication April 5, 2022.

*Correspondence: jblynch@g.ucla.edu

Jonathan B. Lynch's present address is Department of Integrative Biology and Physiology, University of California, Los Angeles, Los Angeles, California.

Editor: Takayuki Nishizaka.

https://doi.org/10.1016/j.bpj.2022.04.008

Please cite this article in press as: Lynch et al., Transitioning to confined spaces impacts bacterial swimming and escape response, Biophysical Journal (2022), https://doi.org/10.1016/j.bpj.2022.04.008

Swimming and reorientation in bulk fluid by flagellated bacteria are behaviors that have been well studied (13), but recent findings have highlighted that these behaviors do not translate well to swimming in more complex environments. This may be due to changes in environmentally stimulated flagellar organization or activity, or because of interactions between the cell and the physical environment that do not exist in bulk fluid. For example, physical forces cause flagellated swimmers to associate with surfaces (14,15), which has interesting consequences in conditions of heterogeneous surface features (16). Relatedly, changes in the physical environment can also impact behaviors, such as chemotaxis, further highlighting the significance of physical features in processes, such as nutrient acquisition and habitat access (17).

Physical confinement is one important factor that bacteria commonly face during motility, and confinement effects can profoundly alter their trajectory and migration patterns (18); nevertheless, this factor is explicitly excluded from open-space swimming measurements. Even under moderate levels of confinement, swimming microorganisms have been observed to accumulate near a solid surface, produce circular trajectories, and scatter from obstacles (15,19). Recent work revealed that even between bacteria with similar flagellar organizations, there are large variations in swimming tendencies, especially with regard to surface association and confined movement (19). The drastic changes in the behavior of confined bacteria as well as the underlying physical mechanisms are not well understood, and highlight that open-space swimming characterizations will often not accurately generalize to swimming in other physical conditions. Understanding the impact that confinement has on flagellar swimming is especially important for host-associated bacteria, which often navigate tight spaces to reach tissue sites where they will stably colonize their host (20).

The symbiotic marine bacterium *Vibrio (Aliivibrio) fischeri* offers a valuable model for studying the influence that transitioning to confined space has on flagellar swimming. Several strains of this bacterium transit from open ocean water to stably colonize animal hosts, such as the Hawaiian bobtail squid (*Euprymna scolopes*) (21). In the well-characterized squid-Vibrio symbiosis, *V. fischeri* traverses distinct microenvironments before reaching its permanent residence in the deep crypts of the juvenile squid light organ. The penultimate microenvironment *V. fischeri* reaches before the crypts—the so-called bottleneck —can close to widths of less than 2 μm (22,23), preventing most cells from completing this journey. This situation means that, as *V. fischeri* colonizes the squid, it must transition from effectively no confinement to an extremely tight degree of confinement. As flagellar motility has previously been shown to be essential for its symbiotic organ colonization (5,24), and as other *Vibrio* spp. use flagella to colonize similar host tissues with some degree of confinement (25), we reasoned that *V. fischeri* would provide an excellent tool for examining changes in swimming behaviors during transitions between environments of varying confinement.

Here, we use microfluidics, high-speed microscopy, and mathematical modeling to describe the behavior of bacteria swimming into a confined space from an unconfined one. We find that while speed remains nearly constant across conditions, cells swimming under confined conditions tend to swim straighter than less-confined cells. This adjustment in swimming directionality is paired with a delayed frequency of sharp reversals. Together, these new behaviors promote an exiting of highly confined spaces, an outcome that we observed through both simulation and experimental observation. We also found that this apparent aversion to confinement can be counterbalanced with chemoattraction, leading to a stable spatial organization of cells. These factors may explain a critical behavior used by bacteria while they navigate between free-living and symbiotic habitats.

MATERIALS AND METHODS

Bacterial preparation

V. fischeri wild-type strain ES114 (26) was grown in LBS medium ([pH 7.5], 10 g L^{-1} tryptone, 5 g L^{-1} yeast extract, 342 mM NaCl, 20 mM Tris (27)) at 28°C. To label cells with GFP, plasmid pVSV102 (Kan^r, (28)) was conjugated into *V. fischeri* using a previously described protocol (29). GFP-expressing cells were isolated on LBS plates containing kanamycin (50 μg mL^{-1}) and stored in 25% glycerol at −80°C.

For experimental conditions, individual colonies of GFP-labeled *V. fischeri* were placed in 1 mL of SWT medium (70% ocean water, 5 g L^{-1} tryptone, 3 g L^{-1} yeast extract, 32.5 mM glycerol (29)) for 90 min at 28°C; these cells were pelleted at 8000 × *g* for 5 min. The supernatant was removed, and the cells were resuspended in 1 mL of filter-sterilized ocean water (FSOW), and left at room temperature throughout imaging.

For chemoattraction experiments, L-serine was dissolved in FSOW to a final concentration of 40 mM, and added outside of the end of a capillary tube.

Fluorescence open-space imaging

V. fischeri ES114 was subcultured from a single colony as described above, pelleted, and resuspended in FSOW, then stained using FM 4-64FX (Thermo Fisher, Waltham, MA) according to previous protocols (10). About 10 μL of cell suspension was spotted inside of a fingernail polish ridge forming a square on a clean glass slide, and was sealed under a glass coverslip. Cells were imaged on a Nikon Eclipse Ti TIRF microscope using a 100× NA 1.5 TIRF objective (Nikon, Melville, NY) at 3 frames s^{-1} rate with a Cascade 512B EMCCD camera (Photometrics, Tucson, AZ). FM 4-64FX was excited at 532 nm (∼10% laser power) and the emission was spectrally filtered (ZET532-10/ZT594rdc/ET645-75m; Chroma, Bellows Falls, VT) within the infinity space before reaching the detector.

Motility measurements

Bacterial motility experiments were performed in two different settings: 1) dead-end microfluidic channels and 2) pulled-glass capillaries. For channel experiments, a microfluidic device made of polydimethylsiloxane contained a straight-flow channel with width × height of 200 × 100 μm. At the middle of the channel, an array of narrow dead-end pores is laid perpendicular to the flow channel (see, e.g., (30)). The height of the dead-end channels was either 2 or 10 μm, while the width and the length of

Please cite this article in press as: Lynch et al., Transitioning to confined spaces impacts bacterial swimming and escape response, Biophysical Journal (2022), https://doi.org/10.1016/j.bpj.2022.04.008

the channels were kept at 45 and 400 μm, respectively. The motion of bacteria was observed using an inverted optical microscope (IX73, Olympus, Center Valley, PA) and a high-speed camera (Phantom Miro M110, Vision Research, Wayne, NJ). For the capillary experiments, pulled-glass microcapillaries (World Precision Instruments, Sarasota, FL) with a tip-opening diameter of between 1 and 10 μm were placed in a closed chamber that was filled with filtered-sterilized seawater. The other end of the capillary was connected to a suspension of *V. fischeri*, which is placed on a vertical stage. By controlling the height of the reservoir, the background fluid flow can be mitigated. A small drop of 40 mM serine (31) was placed in the chamber at the tip of the capillary, and the motion of bacteria was observed using an inverted fluorescent microscope (DMi8, Leica, Buffalo Grove, IL).

Image processing and data analysis

Cellular positioning was manually tracked at a rate of 25 frames s^{-1} by three independent researchers using Tracker 5.1.5 (https://physlets.org/tracker/). The *x*-*y* coordinates were exported and used to calculate position, speed, and angle with MATLAB (Mathworks, Portola Valley, CA).

Computational modeling

We performed simulations of a dilute suspension of bacteria swimming independently in two dimensions. Each bacterium was assumed to swim at a constant speed ($U = 50$ μm s^{-1}) in a direction that changes randomly due to thermal fluctuations and reversals. The reversals are modeled as a stochastic process such that, after a fixed refractory period of either 0 or 0.5 s when no reversal occurs, the next reversal follows randomly with mean rate $f = 3$ s^{-1} and independently of the time since the refractory period. Otherwise, the direction changes continuously with rotational diffusion coefficient $D_r = 0.5$ or 1.0 rad^2 s^{-1}. The resultant trajectories and directional changes were simulated in MATLAB (see below).

Two-dimensional space

We consider a dilute suspension of bacteria moving horizontally in two dimensions. Minor vertical displacements in the third dimension were neglected because 1) the vertical displacements were not tracked in our experiments and 2) the channels constrained the bacteria to move primarily in the horizontal directions, especially in the channels with 2 μm spacing between the ceiling and the floor. The vast majority of bacteria remained far away from the side walls and the ends of the channels. Thus, they were neglected in the model.

Stochastic reversals

The trajectories of *V. fischeri* are characterized by "run-and-reverse" dynamics consisting of relatively straight runs intervened by sudden reversals in swimming direction. The duration of each run is commonly assumed to have an exponentially decaying distribution, which arises if reversals occur randomly at some mean rate f and independently of the time since the last reversal. However, our observations showed that bacteria in 2 μm channels have smaller occurrences of short runs (Fig. 2E), suggesting that some refractory period is needed after each reversal before the next reversal can occur. This motivated us to introduce a refractory period with no reversal for a fixed duration T, which was set to 0 or 0.5 s in 10 or 2 μm channels, respectively. Following this refractory period, the next reversal was assumed to occur randomly with mean rate $f = 3$ s^{-1}. The reversals, which consisted of changes in swimming direction by a distribution of angles ranging from approximately 120° to 180°, were simplified with a fixed and instantaneous directional change of 180° in our model.

Thermal fluctuations

Temporal changes in position and orientation of the bacteria were influenced significantly by thermal fluctuations. Our observations show that the swimming direction, which is expected to align approximately parallel to the long axis of the cell body, fluctuated considerably over time. By focusing on small angular displacements less than 120° within 0.08 s to filter out the effects of reversals, and inspecting the linear growth in mean-square angular displacements with time due to thermal fluctuations, we estimated the rotational diffusion coefficient to be approximately 3.8 or 2.0 s^{-1} in 10 or 2 μm channels, respectively. The actual coefficients are likely to be smaller because flagellar activity may have produced additional directional changes. Nevertheless, the rotational diffusion coefficient is expected to be smaller in 2 than 10 μm channels because rotating bacteria are resisted by increased viscous drag in tighter confinement. To study the effects of reduced rotational diffusion in tighter confinement, we considered bacteria with a characteristic rotational diffusion coefficient of $D_r = 1.0$ s^{-1} and reduced it by a factor of 2 in our model. The model neglected the effects of translational diffusion on the bacterium's position, as the position was impacted more strongly by swimming. The swimming speed, which fluctuated with time in our experiments, was kept fixed at $U = 50$ μm s^{-1}.

Simulations

We simulated the bacterial dynamics using a discrete-time stochastic model. The model predicts the position and orientation of each bacterium using three time-dependent variables (X, Y, and Θ), where X and Y denote the coordinates along and across the channel, respectively, and Θ denotes the angle in radians between the instantaneous swimming direction and the axis along the channel. The positions and directions were marched forward in time using the set of Langevin equations:

$$X[t+\Delta t] = X[t] + U\cos[\Theta[t]]\Delta t \quad (1)$$

$$Y[t+\Delta t] = Y[t] + U\sin[\Theta[t]]\Delta t \quad (2)$$

$$\Theta[t+\Delta t] = \Theta[t] + (2D_r\Delta t)^{1/2}A[t] + \pi B[t], \quad (3)$$

where $\Delta t = 0.04$ s is the time step, and A and B are pseudorandom numbers generated in MATLAB. We set $A = 0$ for the duration in time $T + G$ after each reversal, where T is the fixed refractory period, and G is the variable time until the next reversal after the refractory period. The variable times G have a geometric distribution with small probability $p = f\Delta t = 0.02$, which ensured that reversals occur with mean rate f and independently of the time after the refractory period. At the time step of reversal, we set $A = 1$. Pseudorandom numbers B have a standard normal distribution to account for thermal fluctuations. We simulated $N = 100$ bacteria, all starting with $X = Y = \Theta = 0$ at time $t = 0$, and terminating at time $t = 10$ s. Any bacterium with $X < 0$ was marked as escaped. Bacteria in 2 and 10 μm channels were simulated separately by adjusting the parameters D_r and T, keeping the other parameters U and f fixed. The parameter values used in the simulations are shown in the table below. These values are comparable in order of magnitude with those estimated empirically using our experimental data.

Table 1 presents parameter values used in computer simulations.

Statistical analysis

All statistics were performed in MATLAB (The MathWorks, Portola Valley, CA). Error bars presented represent mean ± SD.

RESULTS

Physical confinement alters swimming behavior

V. fischeri displays a generally nondirectional pattern of swimming in open space (Video S1); however, due to previously described work finding that asymmetric physical

Please cite this article in press as: Lynch et al., Transitioning to confined spaces impacts bacterial swimming and escape response, Biophysical Journal (2022), https://doi.org/10.1016/j.bpj.2022.04.008

TABLE 1 Parameter values used in computer simulations

Confinement gap (μm)	2	10
Rotational diffusion coefficient D_r (1/s)	0.5	1.0
Refractory period after each reversal, T (s)	0.5	0.0
Mean reversal rate after refractory period, f (1/s)	3	3
Swimming speed U (μm/s)	50	50

environments promote spatially organized bacterial populations (32), we hypothesized that confinement similar to that seen during colonization would stimulate a more directed or organized swimming activity. To test the effects that physical confinement had on bacterial swimming behavior, we designed dead-end microfluidics devices with varying levels of two-dimensional confinement (Fig. 1 *A*). These devices contained a central "open" chamber, in which there is effectively no confinement in any direction, as well as several perpendicular "confined" channels, in which there is little confinement in the *x*-*y* direction, but the bacteria are confined on the top and the bottom (*z* direction) (Fig. 1 *A*). Importantly, there was no directional background flow throughout the microfluidic apparatus (30).

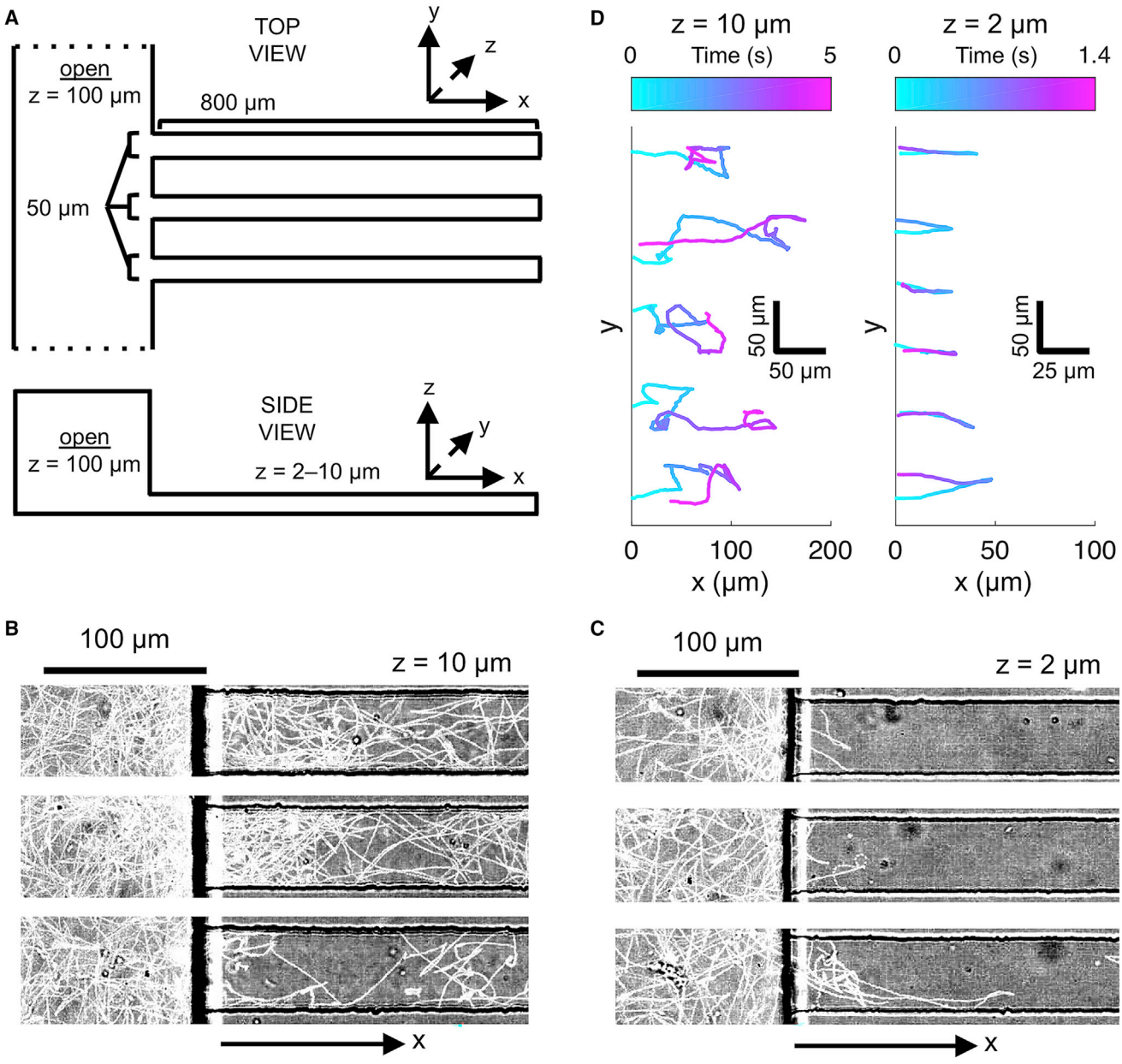

FIGURE 1 Confinement promotes channel escape in *V. fischeri*. (*A*) Schematic of confinement channels for 2 and 10 μm confinement. (*B*) Collapsed traces of *V. fischeri* swimming under 10 μm *z* confinement over 10 s. (*C*) Collapsed traces of *V. fischeri* swimming under 2 μm *z* confinement over 10 s. Left of vertical black lines is open chamber, right of black lines are confined channels. (*D*) Selected traces of *V. fischeri* cells entering noted *z* confinement. Color denotes time in seconds.

Please cite this article in press as: Lynch et al., Transitioning to confined spaces impacts bacterial swimming and escape response, Biophysical Journal (2022), https://doi.org/10.1016/j.bpj.2022.04.008

We measured swimming under varying confinement after loading these devices with a suspension of the well-studied *V. fischeri* isolate ES114 (26) in particle-free FSOW. This medium choice was made to minimize consumable nutrients and the potential production of chemotactic gradients. Previous electron microscopy images showed that the comma-shaped cell bodies of intact *V. fischeri* cells are ~0.6–1 μm wide (33,34), so, to create relatively confined and unconfined environments, we used devices with two z heights, defining the two-sided confinement spacing: 10 μm, in which *V. fischeri* would be relatively less confined, and 2 μm, in which *V. fischeri* would be tightly confined. We were surprised to discover that *V. fischeri* cells displayed distinctive swimming behaviors as they moved from the open chamber into the differently confined channels (Videos S2 and S3). Specifically, while cells entering the 10 μm channels swam freely throughout the channel (Fig. 1 *B*), cells entering the tightly confined 2 μm channels quickly and efficiently exited the channels (Fig. 1 *C*). These contrasting behaviors were even more marked when we tracked individual bacteria in each confinement (Fig. 1 *D*).

Confinement reduces residency

We tracked >300 individual trajectories of *V. fischeri* cells entering either confined or unconfined channels, and quantified differences in swimming parameters between cells entering these two differently confined channels. *V. fischeri* moving into confined channels penetrate more shallowly (Fig. 2 *A*) and spend less time in the channels (Fig. 2 *B*). We found minimal differences in speed between the two confinement states (Fig. 2 *C*). We also did not find a difference between the entering and exiting speeds (Fig. 2 *D*), or between cells that had recently entered the channels and those that had been in the channels for a while (Fig. 2, *C* and *D*).

Confinement delays reversals

We next aimed to uncover what factors contributed to the stark divergence in swimming behavior as cells entered differently confined environments. One important distinction that emerged from comparing bacteria swimming in 2 and 10 μm channels is in the "run duration," or the time interval between sharp reversals. The reversals were noted when the swimming direction changed by more than 120° within 80 ms. We observed that bacteria entering the 2 μm channels had a reversal pattern distinct from those entering 10 μm channels. Specifically, in the less-confined condition, there was an exponential decrease in the frequency distribution of run durations (exponential fit, 10 μm channel $R^2 = 0.93$; 49.4% of runs <0.4 s) indicating a random and equally distributed pattern of sharp reversals (35) (Figs. 2 *E* and S1). However, in the 2 μm channels,

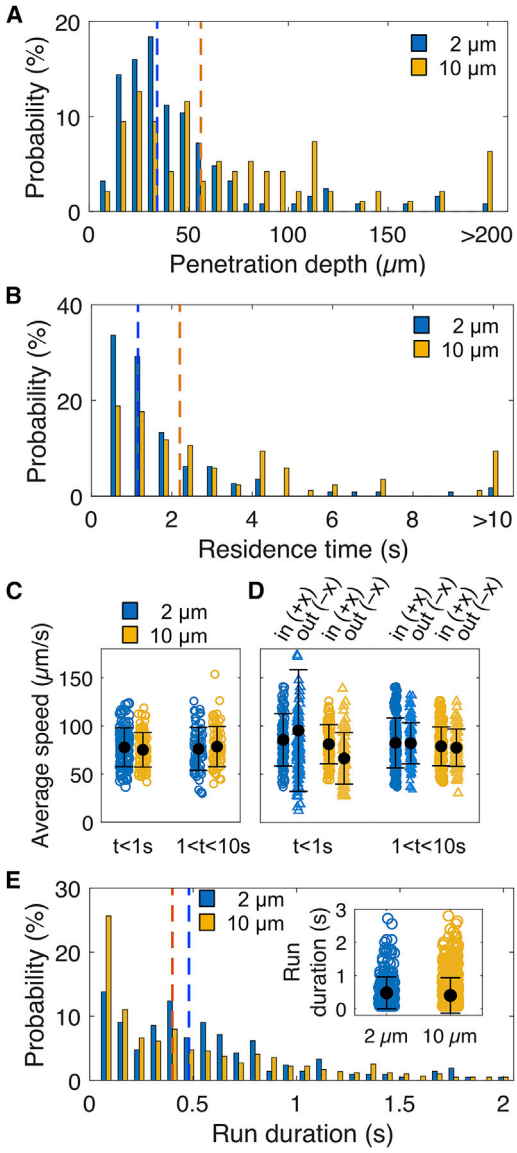

FIGURE 2 Confinement reduces penetrance and residence time of *V. fischeri*. (*A*) Maximum penetration depth into channels of *V. fischeri* under 2 or 10 μm confinement. Dotted lines represent median. (*B*) Channel persistence time of *V. fischeri* under 2 or 10 μm confinement. Dotted lines represent median. (*C*) Average per cell swimming speed of *V. fischeri* during the $t = 0$–1 s or $t = 1$–9 s of each cell entering the confinement channel. Black dots and error bars = mean ± SD. (*D*) Average per cell speed of *V. fischeri* as it swims into (*circles* on left, positive x direction) or out of (*triangles* on right, negative x direction) confinement channels during the $t = 0$–1 s or $t = 1$–9 s intervals. Black dots and error bars = mean ± SD. (*E*) Histogram of run duration before a sharp (>120°) reversal of *V. fischeri* under 2 or 10 μm confinement. Dotted lines represent median. Inset shows individual values, with black dots and bars representing mean ± SD. For all panels: blue, 2 μm; orange, 10 μm.

while quick reversals were relatively infrequent, there was a relative peak of reversals after ~0.5 s, followed by a random reversal frequency similar to those seen in 10 μm channels (exponential fit, 2 μm channel $R^2 = 0.72$; 36.2% of runs <0.4 s) (Fig. 2 *E*). These data indicate that confined

Please cite this article in press as: Lynch et al., Transitioning to confined spaces impacts bacterial swimming and escape response, Biophysical Journal (2022), https://doi.org/10.1016/j.bpj.2022.04.008

cells display a temporary decrease in reversal frequency, resembling a quasi-"refractory" period between reversals, during which they tend to have a period of longer swimming runs, both after entering the channels and between reversals.

Confinement reduces directional deviation

In addition to a discrepancy in reversal patterns between cells in the 2 and 10 μm channels, we hypothesized that a cell rotating around the vertical z axis is expected to experience increased viscous drag in tighter gaps, resulting in a lower rotational diffusion coefficient. To measure this, we measured the bacterial swimming direction, which is predicted to change randomly over time due to thermal fluctuations in the surrounding fluid. Our analysis revealed that the bacteria undergo both small and large directional changes, the latter due primarily to sharp reversals. To estimate the rotational diffusion coefficient arising solely from thermal fluctuations, we removed sharp reversals (as defined earlier, directional changes exceeding 120° within 80 ms), and considered the mean of the square of the cumulative directional change over time (Fig. 3 *A*). This analysis revealed that confined cells displayed lower changes in directional reorientation than unconfined cells (rotational diffusion coefficient [D_r]: $D_{r,10\mu m} = 3.8$ rad^2 s^{-1}; $D_{r,2\mu m} = 2.0$ rad^2 s^{-1}). From these data we concluded that confined cells exhibited straighter swimming trajectories than their unconfined counterparts (Fig. 3 *A*). We did not find evidence of either confinement-based orientation that could steer the bacteria toward an exit, or any association

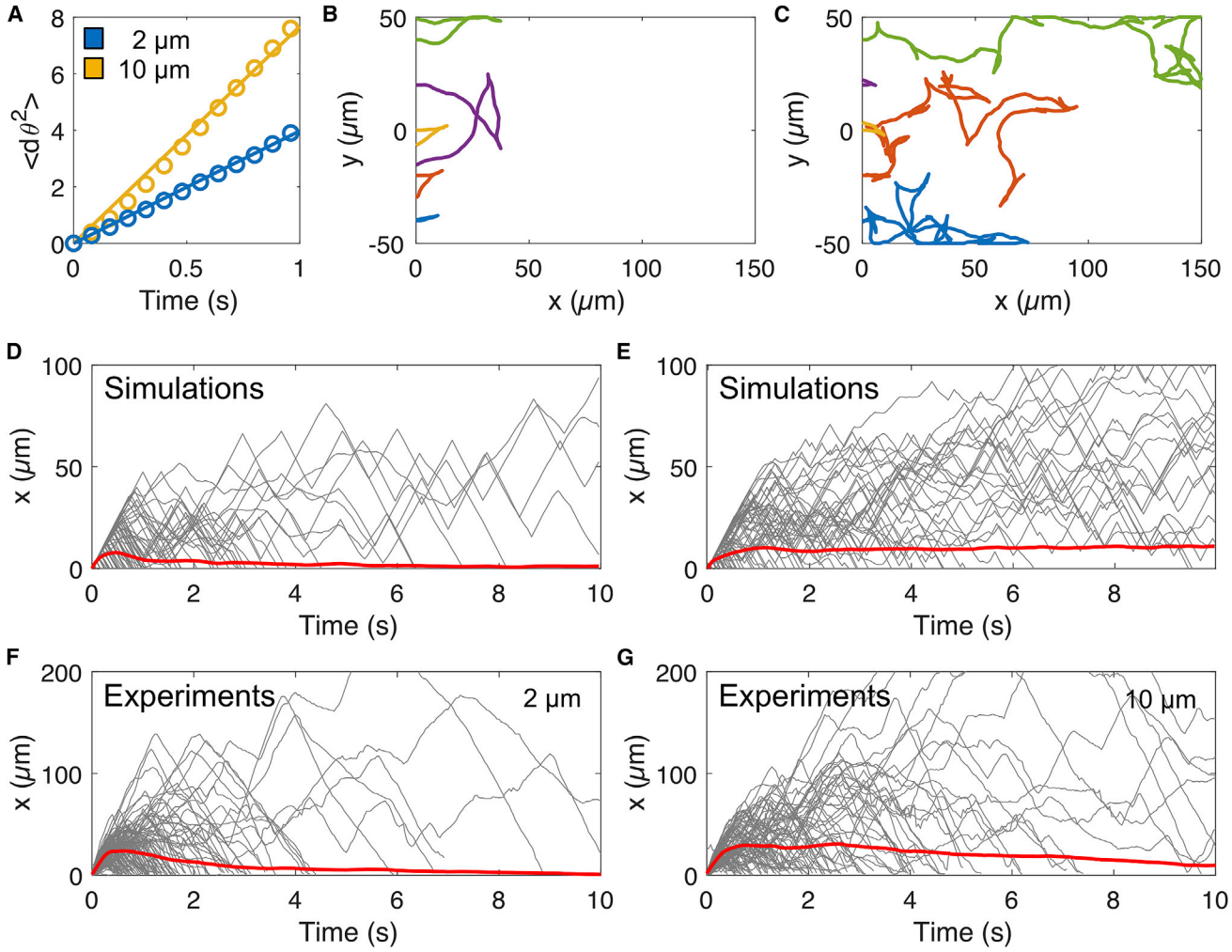

FIGURE 3 Confined cells have lower rotational diffusion, facilitating escape behavior. (*A*) $<d\theta^2>$ over time of cells in 10 μm (*orange*) or 2 μm (*blue*) confined channels. The slope of these lines approximates $2D_r$. Circles represent experimental data, line is best linear fit. (*B*) Simulation of cells swimming with a rotational diffusivity (D_r) of 0.5 rad^2 s^{-1} and a 0.5 s delay between periods of random reversal, approximating activity seen in 2 μm channels. (*C*) Simulation of cells swimming with a D_r of 1 rad^2 s^{-1} and random reversal frequency, approximating activity seen in 10 μm channels. (*D*) Spatiotemporal plots of *x* penetrance over time for cells in (*B*). (*E*) Spatiotemporal plots of *x* penetrance over time for cells in (*C*). (*F*) Experimental spatiotemporal diagrams for *V. fischeri* swimming into a 2 μm confinement chamber. (*G*) Experimental spatiotemporal diagrams for *V. fischeri* swimming into a 10 μm confinement chamber. In (*B*) and (*C*), each line represents the trajectory of one simulated cell. In (*D*)–(*G*), each black line represents the *x* position of one cell, and red lines represent the mean position of all cells that have entered the channel, including those that exit during the experiment.

Please cite this article in press as: Lynch et al., Transitioning to confined spaces impacts bacterial swimming and escape response, Biophysical Journal (2022), https://doi.org/10.1016/j.bpj.2022.04.008

between angle positioning and swimming speed (Fig. S2 *A*). Specifically, we observed no association between orientation angle and angle change (Fig. S2, *B* and *C*) or between orientation angle and speed change (Fig. S2, *D* and *E*) in either the confined or unconfined channels.

Long-term implications of confinement

To better understand the long-term implications of the delayed reversals and the reduced rotational diffusion coefficient of bacteria in the relatively tighter confinement, we developed a simplified model to simulate the bacteria swimming with these differing traits (see Materials and methods). By varying D_r and the delay in reversals while keeping all other parameters fixed, we found a drastic qualitative difference in swimming behavior, consistent with our experimental observations of the trajectories over short times (Fig. 3, *B* and *C*). Over longer times, the simulations predicted the majority of bacteria to escape, but only after reducing the rotational diffusion and delaying reversals in combination (Fig. 3, *D* and *E*); singly reducing rotational diffusion or delaying reversals did not lead to confinement avoidance (Fig. S3). When we compared these simulated results with those from our experimental findings, we found similar residency times and escape behavior (Fig. 3, *F* and *G*). We may interpret the time to escape as a first passage time of a cell undergoing effective translational diffusion (e.g., (36)). Since the bacteria with reduced rotational diffusion and delayed reversals are predicted to have a higher translational diffusivity (37), we can expect them to disperse more quickly and appear to escape from tighter confinement. While other factors may contribute to the escape response, our simulations demonstrate that changes in rotational diffusivity and reversal frequency are sufficient to result in confinement-associated escape behavior.

Confinement-based swimming can be counterbalanced by chemotactic cues

After demonstrating the confinement-avoidance swimming behavior, we sought to explore how this behavior influenced another known modulator of swimming behavior: chemotaxis. For these experiments, we used serine, which is a strong chemoattractant for *V. fischeri* (31). To allow us to simultaneously confine the cells while applying the attractant, we confined the bacteria with precise-diameter glass capillaries (see Materials and methods) rather than dead-end channels. Suspensions of *V. fischeri* were loaded into the capillaries and, after minimizing background flow, we monitored the distribution of the cells inside capillaries of different terminal diameters after addition of the chemoattractant outside the capillary tip (see comparison before and after chemoattractant addition in Fig. S4). In tightly confined capillaries (1 or 2 μm minimum diameter), cells avoided the most confined region (tip) of the capillary, mirroring what we saw in our dead-end channels (Videos S4, S5, and S6). Even with the presence of chemoattractant in the external fluid, cells avoided the tip, rarely passing through these regions despite the physical clearance to do so (Fig. 4, *A* and *B*). Conversely, cells experiencing less confinement readily left the capillaries and swam toward the chemoattractant outside the tip (Fig. 4 *C*). This led to high concentrations of cells accumulating close to—but not at—the confined capillary tips, versus cellular density

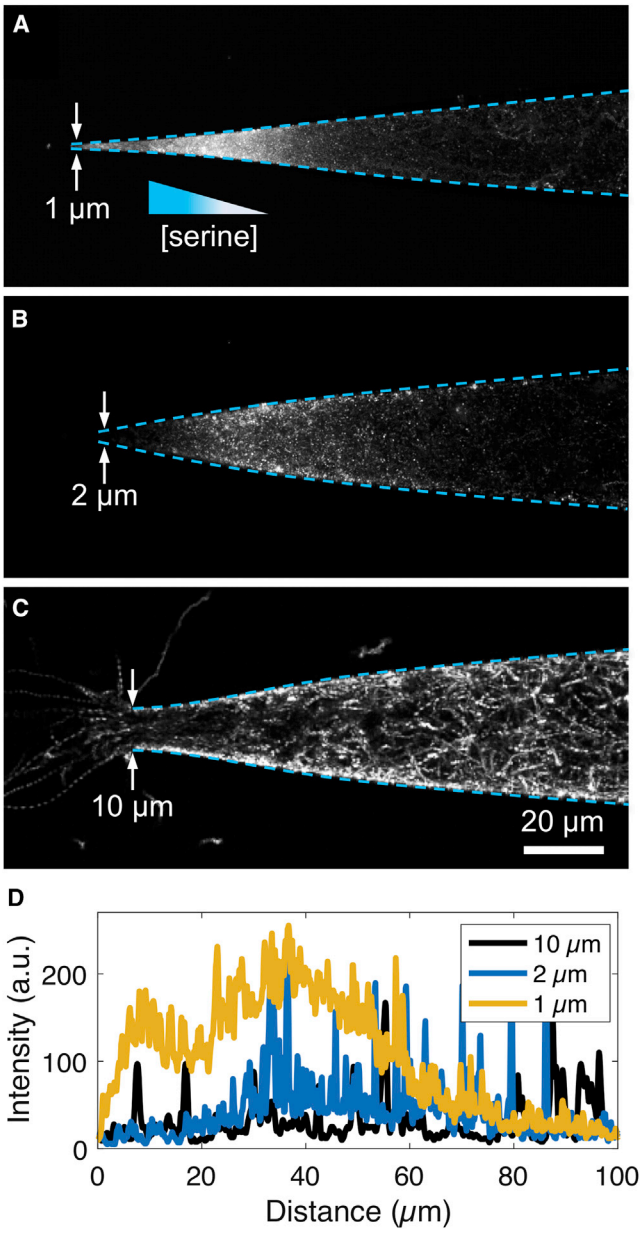

FIGURE 4 Chemoattraction counterbalances avoidance of confined spaces. Collapsed images from times lapse videos of GFP-labeled *V. fischeri* in glass capillaries with inner tip diameter of 1 μm (*A*), 2 μm (*B*), or 10 μm (*C*) after external addition of chemoattractant. Dotted cyan lines indicate edges of microcapillary. (*D*) Fluorescence intensity plot along the centerline of the capillary starting from the tip entrance into the capillary.

Please cite this article in press as: Lynch et al., Transitioning to confined spaces impacts bacterial swimming and escape response, Biophysical Journal (2022), https://doi.org/10.1016/j.bpj.2022.04.008

equilibrium maintained by accumulation and escape of cells in the unconfined tips (Fig. 4 *D*).

DISCUSSION

The data presented here reveal that tight physical confinement can alter bacterial swimming behavior and long-term distribution by reducing directional fluctuations and delaying reversals. These experiments demonstrate that confinement interactions have profound implications on bacterial behavior, and may shape the patterns of motility during habitat transitions, such as those that occur during the initiation of symbiotic associations with animal and plant hosts.

The reversals we tracked under confined conditions could be the result of 1) the run-reverse activity used by many marine bacteria (38), 2) the run-reverse-flick method employed by other *Vibrio* species (39), or 3) flagellar wrapping, all of which allow quick, sharp-angle changes in swimming trajectories (11). Wrapping has been described previously in *Shewanella* sp., *Burkholderia* sp., and *V. fischeri* (10), and could result, at least partially, from interactions between the environment and the physical structure of the flagellar filament and its constituent flagellin proteins (40). The *V. fischeri* genome encodes at least five flagellin genes (41) and, as the timescale of reversal is too short to result from proteomic remodeling of these flagella (42), the specific individual combination of these flagellins could promote or inhibit the structural dynamics required for wrapping, potentially explaining some heterogeneity among cells that quickly reversed rather than persisted in confinement. Also, our measurements showed that confined cells swam forward and backward at similar speeds, whereas previous investigation of wrapping and run-reverse-flick behaviors has shown that these cells swim at different speeds when going forward and backward (11,43). Interestingly, a previous report has also described a difference in trajectory curvature between forward and reverse swimming, especially near a single surface (43). As we did not observe a noticeable difference in translational or angular speed by confined *V. fischeri* before or after reversals, two-sided confinement may balance out differences between forward and reverse swimming, potentially influencing reversals, escape behavior, and other directional movement (44–47).

Importantly, the speed and angle of reversals we describe in this work appear to be faster than either physically guided motor remodeling (48,49) or tumbles (1,50,51), suggesting that active responses from internal cellular responses are not driving these alterations in swimming and reversal behavior. Instead, we suspect that passive reshaping of the flagellum (i.e., not requiring changes in protein expression or motor direction) in response to confinement-induced physical conditions leads to confinement avoidance. In addition, the transition between these passive flagellar organizations may explain the quasi-refractory period we described; there may be a delay in reversals because of the time it takes to move from one flagellar organization to another. Future research into the specific cellular organization of escaping cells will better connect flagellar organization and this novel swimming behavior.

The confined swimming behavior we observed may be selected for among bacterial species that experience confinement as a common part of their lifestyles. By preferentially reversing when confinement increases, cells could escape from places in which they might become stuck. There may even be a critical confinement point beyond which bacteria, especially rod- or comma-shaped bacteria, such as *V. fischeri*, may not be physically able to tumble or flick to facilitate an escape because of their shape and/or the length of their flagella. Such a constraint is exacerbated in bacteria, such as *V. fischeri*, that can also produce extracellular capsule or polysaccharides, increasing their effective dimensions in certain environments (52,53). These cells might avoid immobilization by quickly swimming away from tightly confined spaces and/or by wrapping their flagella to reduce their spatial footprint while swimming. In symbioses between flagellated bacteria and hosts, avoidance of being physically trapped could benefit both the bacterium and the host; if bacteria become trapped during colonization, they would no longer be able to swim toward favorable environments, while the host would experience clogging of bacteria-colonized tissues. In addition, the confinement-avoidance behavior we describe could occur in addition to or instead of other confinement-associated swimming motility, such as hopping/trapping seen in *E. coli* (16), providing cells with multiple means to navigate complex environments.

For bacteria like *V. fischeri*, which also must proceed through tightly confined spaces on the way to their target tissue, the balance between confinement-avoidance and positive taxis (e.g., attraction to host-derived nutrients) may facilitate a stochastic procession through tightly confined spaces. This phenomenon may explain some of the extreme bottlenecking of *V. fischeri* cells on the way to the light organ crypts, which results in very few cells actually being able to colonize the symbiotic organ; a small number of cells may be able to process through the confined tissue before reversing, whereas the vast majority escape before passing through the confined region (54). Similar dynamics could play out in other symbiosis with tightly confining symbiotic tissues (55,56), or with bacteria shaped like *V. fischeri*, including several pathogens (57). The combination of straighter swimming trajectories and increased escape activity could promote behavior where cells either make it through a tightly confined space to their target environment, or back out before they get stuck. This same principle could be applied to sort or separate cells based on their motility; physically confined environments could be experimentally shaped to selectively enrich for or against cells with this type of confinement-associated swimming behavior. Previously, similar physical heterogeneity has been shown to

Please cite this article in press as: Lynch et al., Transitioning to confined spaces impacts bacterial swimming and escape response, Biophysical Journal (2022), https://doi.org/10.1016/j.bpj.2022.04.008

powerfully guide bacterial sorting (32). Our findings could inform the creation of apparatuses that spatially organize swimming cells by directing their confinement, providing a simple means to shape bacterial populations and communities. Our results also open the door for further exploration of the physical and biological determinants of confined swimming, holding major implications for fields such as host-microbe symbiosis and microbial biophysics.

While our findings focus on one well-studied symbiotic bacterium, it is equally important to explore the effects of environmental confinement on other symbiotic and nonsymbiotic bacteria. We predict that the physical forces driving the confinement escape behavior are conserved across bacteria with similar shape and motility traits as *V. fischeri* (flagellated, rod- or comma shaped, etc.), and that our findings are generalizable to a wide-range of biological situations. Although we focused on overall cellular behavior, it remains to be seen how specific structures—namely, flagella— influence motility under confined conditions. Future experiments that describe the positioning and activity of flagella under these conditions would greatly inform the specific behavioral and physical drivers of confinement avoidance.

CONCLUSION

Our findings open new questions about how bacteria and other flagellated cells navigate their physical environments, and how they modify their behaviors according to their surroundings. Questions remain about how different bacteria respond to confinement, the physical and biological factors that promote or reduce this escape behavior, and the downstream consequences of swimming modulation in response to confinement. These findings could explain complex interactions between bacteria and their environments, providing insights into diverse fields, such as biofouling and multispecies symbiosis.

Data and code availability

All code is available at https://github.com/jblynch123/Vf-confinement. Experimental materials are available upon reasonable request to the corresponding author.

SUPPORTING MATERIAL

Supporting material can be found online at https://doi.org/10.1016/j.bpj.2022.04.008.

AUTHOR CONTRIBUTIONS

Conceptualization, J.B.L., S.S., and D.T.; methodology, J.B.L., N.J., S.S., and D.T.; software, S.S. and D.T.; investigation, J.B.L., N.J., S.S., and D.T.; visualization, J.B.L., S.S., and D.T.; supervision, J.B.L., M.M.-N., E.G.R., S.S., and D.T.; writing – original draft, J.B.L., S.S., and D.T.; writing – review & editing, J.B.L., N.J., M.M.-N., E.G.R., S.S., and D.T.

ACKNOWLEDGMENTS

This work was supported by National Institutes of Health grant F32 GM119238 (to J.B.L.), a Ford Foundation Postdoctoral Fellowship (to J.B.L.), a C-MĀIKI seed grant from the University of Hawai'i at Mānoa (to J.B.L. and D.T.), and National Institutes of Health grant R01 GM135254 (to E.G.R. and M.M.-N.).

REFERENCES

1. Berg, H. C., and D. A. Brown. 1972. Chemotaxis in *Escherichia coli* analysed by three-dimensional tracking. *Nature.* 239:500–504.
2. Lauga, E. 2016. Bacterial hydrodynamics. *Annu. Rev. Fluid Mech.* 48:105–130.
3. Medina, A. A., R. M. Shanks, and D. E. Kadouri. 2008. Development of a novel system for isolating genes involved in predator-prey interactions using host independent derivatives of *Bdellovibrio bacteriovorus* 109J. *BMC Microbiol.* 8:33.
4. Huang, J. Y., E. G. Sweeney, M. R. Amieva…, 2015. Chemodetection and destruction of host urea allows *Helicobacter pylori* to locate the epithelium. *Cell Host Microbe.* 18:147–156.
5. Brennan, C. A., M. J. Mandel, …, E. G. Ruby. 2013. Genetic determinants of swimming motility in the squid light-organ symbiont *Vibrio fischeri*. *Microbiologyopen.* 2:576–594.
6. Guentzel, M. N., and L. J. Berry. 1975. Motility as a virulence factor for *Vibrio cholerae*. *Infect. Immun.* 11:890–897.
7. Berg, H. C. 2003. The rotary motor of bacterial flagella. *Annu. Rev. Biochem.* 72:19–54.
8. Son, K., J. S. Guasto, and R. Stocker. 2013. Bacteria can exploit a flagellar buckling instability to change direction. *Nat. Phys.* 9:494–498.
9. Hintsche, M., V. Waljor, …, C. Beta. 2017. A polar bundle of flagella can drive bacterial swimming by pushing, pulling, or coiling around the cell body. *Sci. Rep.* 7:16771.
10. Kinosita, Y., Y. Kikuchi, T. Nishizaka…, 2018. Unforeseen swimming and gliding mode of an insect gut symbiont, *Burkholderia sp*. RPE64, with wrapping of the flagella around its cell body. *ISME J.* 12:838–848.
11. Kühn, M. J., F. K. Schmidt, …, K. M. Thormann. 2017. Bacteria exploit a polymorphic instability of the flagellar filament to escape from traps. *Proc. Natl. Acad. Sci. U S A.* 114:6340–6345.
12. Reichhardt, C. J. O., and C. Reichhardt. 2017. Ratchet effects in active matter systems. *Annu. Rev. Condens. Matter Phys.* 8:51–75.
13. Taute, K. M., S. Gude, …, T. S. Shimizu. 2015. High-throughput 3D tracking of bacteria on a standard phase contrast microscope. *Nat. Commun.* 6:8776.
14. Vigeant, M. A. S., R. M. Ford, L. K. Tamm…, 2002. Reversible and irreversible adhesion of motile *Escherichia coli* cells analyzed by total internal reflection aqueous fluorescence microscopy. *Appl. Environ. Microbiol.* 68:2794–2801.
15. Lauga, E., W. R. DiLuzio, …, H. A. Stone. 2006. Swimming in circles: motion of bacteria near solid boundaries. *Biophys. J.* 90:400–412.
16. Bhattacharjee, T., and S. S. Datta. 2019. Bacterial hopping and trapping in porous media. *Nat. Commun.* 10:2075.
17. Bhattacharjee, T., D. B. Amchin, …, S. S. Datta. 2021. Chemotactic migration of bacteria in porous media. *Biophys. J.* 120:3483–3497.
18. Zhou, S., O. Tovkach, …, O. D. Lavrentovich. 2017. Dynamic states of swimming bacteria in a nematic liquid crystal cell with homeotropic alignment. *New J. Phys.* 19:055006.
19. Tokárová, V., A. Sudalaiyadum Perumal, …, D. V. Nicolau. 2021. Patterns of bacterial motility in microfluidics-confining environments. *Proc. Natl. Acad. Sci. U S A.* 118:e2013925118.
20. Raina, J.-B., V. Fernandez, …, J. R. Seymour. 2019. The role of microbial motility and chemotaxis in symbiosis. *Nat. Rev. Microbiol.* 17:284–294.

Please cite this article in press as: Lynch et al., Transitioning to confined spaces impacts bacterial swimming and escape response, Biophysical Journal (2022), https://doi.org/10.1016/j.bpj.2022.04.008

21. McFall-Ngai, M. J. 2014. The importance of microbes in animal development: lessons from the squid-Vibrio symbiosis. *Annu. Rev. Microbiol.* 68:177–194.

22. Essock-Burns, T., C. Bongrand, …, M. J. McFall-Ngai. 2020. Interactions of symbiotic partners drive the development of a complex biogeography in the squid-Vibrio symbiosis. *mBio.* 11:e00853-20.

23. Essock-Burns, T., B. D. Bennett, E. G. Ruby…, 2021. Bacterial quorum-sensing regulation induces morphological change in a key host tissue during the *Euprymna scolopes-Vibrio fischeri* symbiosis. *MBio.* 12:e0240221.

24. Millikan, D. S., and E. G. Ruby. 2004. *Vibrio fischeri* flagellin A is essential for normal motility and for symbiotic competence during initial squid light organ colonization. *J. Bacteriol.* 186:4315–4325.

25. Echazarreta, M. A., and K. E. Klose. 2019. Vibrio flagellar synthesis. *Front. Cell. Infect. Microbiol.* 9:131.

26. Boettcher, K. J., and E. G. Ruby. 1990. Depressed light emission by symbiotic *Vibrio fischeri* of the sepiolid squid *Euprymna scolopes*. *J. Bacteriol.* 172:3701–3706.

27. Dunlap, P. V. 1989. Regulation of luminescence by cyclic AMP in cya-like and crp-like mutants of *Vibrio fischeri*. *J. Bacteriol.* 171:1199–1202.

28. Dunn, A. K., D. S. Millikan, E. V. Stabb…, 2006. New rfp - and pES213-derived tools for analyzing symbiotic *Vibrio fischeri* reveal patterns of infection and lux expression in situ. *Appl. Environ. Microbiol.* 72:802–810.

29. Lynch, J. B., J. A. Schwartzman, …, E. G. Ruby. 2019. Ambient pH alters the protein content of outer membrane vesicles, driving host development in a beneficial symbiosis. *J. Bacteriol.* 201:e00319-19.

30. Shin, S., E. Um, …, H. A. Stone. 2016. Size-dependent control of colloid transport via solute gradients in dead-end channels. *Proc. Natl. Acad. Sci. U S A.* 113:257–261.

31. DeLoney-Marino, C. R., A. J. Wolfe, and K. L. Visick. 2003. Chemoattraction of *Vibrio fischeri* to serine, nucleosides, and N -acetylneuraminic acid, a component of squid light-organ mucus. *Appl. Environ. Microbiol.* 69:7527–7530.

32. Galajda, P., J. Keymer, …, R. Austin. 2007. A wall of funnels concentrates swimming bacteria. *J. Bacteriol.* 189:8704–8707.

33. Ruby, E. G., and L. M. Asato. 1993. Growth and flagellation of *Vibrio fischeri* during initiation of the sepiolid squid light organ symbiosis. *Arch. Microbiol.* 159:160–167.

34. Vroom, M. M., Y. Rodriguez-Ocasio, J. S. Foster…, 2021. Modeled microgravity alters lipopolysaccharide and outer membrane vesicle production of the beneficial symbiont *Vibrio fischeri*. *NPJ Microgravity.* 7:8.

35. Figueroa-Morales, N., A. Rivera, …, É. Clément. 2020. E. coli "supercontaminates" narrow ducts fostered by broad run-time distribution. *Sci. Adv.* 6:eaay0155.

36. Redner, S. 2001. A Guide to First-Passage Processes, First edition. Cambridge University Press.

37. Krasky, D. A., and D. Takagi. 2018. Diffusion of swimmers jumping stochastically between multiple velocities. *J. Stat. Mech. Theor. Exp.* 2018:103201.

38. Mitchell, J. G., L. Pearson, and S. Dillon. 1996. Clustering of marine bacteria in seawater enrichments. *Appl. Environ. Microbiol.* 62:3716–3721.

39. Xie, L., T. Altindal, …, X.-L. Wu. 2011. Bacterial flagellum as a propeller and as a rudder for efficient chemotaxis. *Proc. Natl. Acad. Sci. U S A.* 108:2246–2251.

40. Kühn, M. J., F. K. Schmidt, …, K. M. Thormann. 2018. Spatial arrangement of several flagellins within bacterial flagella improves motility in different environments. *Nat. Commun.* 9:5369.

41. Ruby, E., M. Urbanowski, D. Millikan…, 2005. Complete genome sequence of *Vibrio fischeri*: a symbiotic bacterium with pathogenic congeners. *Proc. Natl. Acad. Sci. U S A.* 102:3004–3009.

42. Chen, M., Z. Zhao, C.-J. Lo…, 2017. Length-dependent flagellar growth of *Vibrio alginolyticus* revealed by real time fluorescent imaging. *Elife.* 6:e22140.

43. Magariyama, Y., M. Ichiba, …, T. Goto. 2005. Difference in bacterial motion between forward and backward swimming caused by the wall effect. *Biophys. J.* 88:3648–3658.

44. Alirezaeizanjani, Z., R. Großmann, …, C. Beta. 2020. Chemotaxis strategies of bacteria with multiple run modes. *Sci. Adv.* 6:eaaz6153.

45. Antani, J. D., A. X. Sumali, P. P. Lele…, 2021. Asymmetric random walks reveal that the chemotaxis network modulates flagellar rotational bias in *Helicobacter pylori*. *Elife.* 10:e63936.

46. Theves, M., J. Taktikos, …, C. Beta. 2013. A bacterial swimmer with two alternating speeds of propagation. *Biophys. J.* 105:1915–1924.

47. Constantino, M. A., M. Jabbarzadeh, R. Bansil…, 2018. Bipolar lophotrichous *Helicobacter suis* combine extended and wrapped flagella bundles to exhibit multiple modes of motility. *Sci. Rep.* 8:14415.

48. Tipping, M. J., N. J. Delalez, …, J. P. Armitage. 2013. Load-dependent assembly of the bacterial flagellar motor. *mBio.* 4:e00551-13.

49. Wadhwa, N., R. Phillips, and H. C. Berg. 2019. Torque-dependent remodeling of the bacterial flagellar motor. *Proc. Natl. Acad. Sci. U S A.* 116:11764–11769.

50. Alon, U. 1998. Response regulator output in bacterial chemotaxis. *EMBO J.* 17:4238–4248.

51. Lemelle, L., T. Cajgfinger, C. Vaillant…, 2020. Tumble kinematics of *Escherichia coli* near a solid surface. *Biophys. J.* 118:2400–2410.

52. Yip, E. S., K. Geszvain, K. L. Visick…, 2006. The symbiosis regulator RscS controls the syp gene locus, biofilm formation and symbiotic aggregation by *Vibrio fischeri*. *Mol. Microbiol.* 62:1586–1600.

53. Shibata, S., E. S. Yip, K. L. Visick…, 2012. Roles of the structural symbiosis polysaccharide (syp) genes in host colonization, biofilm formation, and polysaccharide biosynthesis in *Vibrio fischeri*. *J. Bacteriol.* 194:6736–6747.

54. Wollenberg, M. S., and E. G. Ruby. 2009. Population structure of *Vibrio fischeri* within the light organs of *Euprymna scolopes* squid from two Oahu (Hawaii) populations. *Appl. Environ. Microbiol.* 75:193–202.

55. Kikuchi, Y., T. Ohbayashi, P. Mergaert…, 2020. *Burkholderia insecticola* triggers midgut closure in the bean bug *Riptortus pedestris* to prevent secondary bacterial infections of midgut crypts. *ISME J.* 14:1627–1638.

56. Ohbayashi, T., K. Takeshita, …, Y. Kikuchi. 2015. Insect's intestinal organ for symbiont sorting. *Proc. Natl. Acad. Sci. U S A.* 112:E5179–E5188.

57. Taylor, J. A., S. R. Sichel, and N. R. Salama. 2019. Bent bacteria: a comparison of cell shape mechanisms in proteobacteria. *Annu. Rev. Microbiol.* 73:457–480.